The Effect of Cold-Worked Ratio on Corrosion Behavior of T8 Tempered Al–Si–Mg/SiC$_p$ Metal Matrix Composites

Burak Dikici [1], Cagri Tekmen [2], Mehmet Gavgali [3], Yoshiki Tsunekawa [2]

[1] Yuzuncu Yil University, Ercis Technical Vocational School of Higher Education, 65400 Ercis-Van, TURKEY
[2] Toyota Technological Institute, Materials Processing Lab, 468-8511, Nagoya, JAPAN
[3] Ataturk University, Department of Mechanical Engineering, 25240 Erzurum, TURKEY

Keywords: *T8 temper, corrosion, metal matrix composite, SiC particle, cold working*

Abstract

The corrosion behaviors of T8 tempered Al–Si–Mg/SiC$_p$ metal matrix composites (MMCs) were investigated in aerated and deaerated 3.5wt% NaCl solutions by potentiodynamic polarization technique in this study. In order to determine the effect of cold work on the electrochemical behavior, the composites were cold-worked to a plastic strain of 4, 6, 10, 25 and 50%. A major change in the corrosion morphologies were observed cold working ratio increased from 4 to 50%. For example, electrochemical analysis indicated that the corrosion current densities (i_{cor}) of 20% vol. SiC composite increased from 0.8 to 5.9 with increasing cold-worked ratio after T8 temper. In addition, we find that there is a significant coloration between corrosion susceptibility and level of cold work.

1. Introduction

Nowadays, aluminum based metal matrix composites (AMMCs) can be strengthen with precipitation hardening (aging), work hardening, reinforcement with intermetallic compounds, solid solution strengthening. One of the main advantages of particle reinforced AMMCs is that billets of the composite can be mechanically processed using technologies developed for monolithic alloys; for example, extrusion, forging or hot and cold rolling. Therefore, the composites are very commonly used in aerospace and automotive industry due to these multi-advantages. However, mechanical properties and the corrosion resistances of these type composites are depending on complex factors such as ratio of deformation and time of ageing besides the microstructure of material. In addition, the factors are also considerable scientific and technical importance. It is accepted that the presence of the reinforcing phase affects both the deformation and ageing behavior of the metal matrix due to the altered re-crystallization kinetics around the reinforcement particles [1–9].

Trowsdale *et .al.* [3] found that the polarization curves of 50% cold-deformed composite after heat treatment were very similar to those in the absence of cold work; in particular, there was no change in the pitting potential. Briefly, according to the authors, the residual stresses and dislocation density are ineffective on the corrosion resistance of Al/SiC composites. Quainoo *et. al.*[6] reported that the precipitation kinetics in alloy during the aged stages, are faster with increasing level of cold work thus less energy will required for the formation of precipitation phases. So, the required activation energy to formation precipitation phases will decrease increasing level of cold work. However, the effects of reinforcements on the precipitation kinetics in MMCs are more complex. Compared to the unreinforced alloys, dislocations created from the thermal mismatch between the matrix and the reinforcements provide additional sites for precipitation and enhance pipe diffusion of solute atoms [8]. For example, the aging mechanism for Al–Si–Mg alloys is developed by controlled decomposition of unstable supersaturated solid solution. The precipitation sequences in the ternary system are GP1$\rightarrow\beta''\rightarrow\beta'\rightarrow\beta$ (Mg_2Si) (Eq. 1) [6, 8]. This phase may alter the corrosion characteristics of the matrix alloy and composite because the Mg concentration in solid solution after aged process is reduced and Mg_2Si precipitations also exhibit cathodic behavior according to Al based matrix alloy [10].

$$Si + 2Mg \rightarrow Mg_2Si \qquad (1)$$

Additionally, according to some research groups, the formation of highly anodic precipitation phases can lead to an increased susceptibility to stress corrosion cracking (SCC) [3, 10–12]. An another possibility, the corrosion resistance of the composites after T8 process may influence due to the increasing of formed vacancies at dislocations and also the reaction products occurred at the Al/SiC interfaces [2]. Published data indicate that the formation of reaction products may have an important influence on the corrosion behavior of the matrix alloy and composites. For example, SiC can react with molten aluminum and producing aluminum-carbide (Al_4C_3), according to the following reaction (Eq. 2) [3, 13]. Composites containing Al_4C_3 are more susceptible to corrosion because it is an extremely brittle phase and water reactive, which may alter the corrosive sensitivity of the composite [14].

$$4Al + 3SiC \rightarrow Al_4C_3 + 3Si \qquad (2)$$

The fabrication method and mechanical properties of AMMCs are now well documented. But, the corrosion susceptibilities of T8 tempered AMMCs have not been fully explained up to now. So it is an urge to understand the effects on corrosion behavior of these composites of relation between cold working and aging. In our previous studies [8, 9], the role of reinforcement volume fraction and aged heat treatment on the corrosion behavior of the composites was determined, respectively. Therefore, the present investigation is aimed to determine pitting resistance and to study the corrosion characteristics of Al–Si–Mg/SiC_P MMCs in T8 heat-treated conditions.

2. Experimental Procedure

Silicon carbide particle (SiC_p) reinforced composites consisting of 10 and 20 vol% SiC_ps are produced by the compocasting technique. In order to determine the effect of cold work on the electrochemical behavior, the composites were cold-worked to a plastic strain of 4, 6, 10, 25 and 50%. In all these type composites, the matrix/reinforcement interfaces is have a significant effect on the composite corrosion performance, so the surface of SiC particles before casting was coated with a thin silicon-dioxide (SiO_2) layer for both improve of adhesion and prevent the formation of Al_4C_3. The details of the production method and T8 process are given in previous studies [8, 15].

The electrochemical behaviours of the composites has been analyzed in aerated and deaerated 3.5 wt.% NaCl aqueous solutions at room temperature in a Pyrex glass cell. In this study, ASTM standards (G 1-03, G5-94) are used both checked of experimental technique and instrumentation and prepared of corrosion test specimens [16, 17]. The all electrochemical measurements were carried out using a PGS95 potentiostat/galvanostat (BANK Inc., Germany). An Ag/AgCl electrode and platinum (Pt.) electrode were used as reference and auxiliary electrodes respectively. The solution was deaerated to remove oxygen with N_2 gas. The deaerated process started at 60 minutes prior to measurement and continued until the end of the experiment. The corroded surfaces of the composites after the corrosion tests are observed by using scanning electron microscopy (SEM). Also, X-ray diffraction (XRD) technique has been used in order to determine phases occurred at the matrix/SiC interface.

3. Results

In aerated conditions, potentiodynamic polarization curves of T8 tempered matrix alloy and 20% SiC composites are given in Fig. 1 which shows the effect of cold-worked ratios on the corrosion resistance.

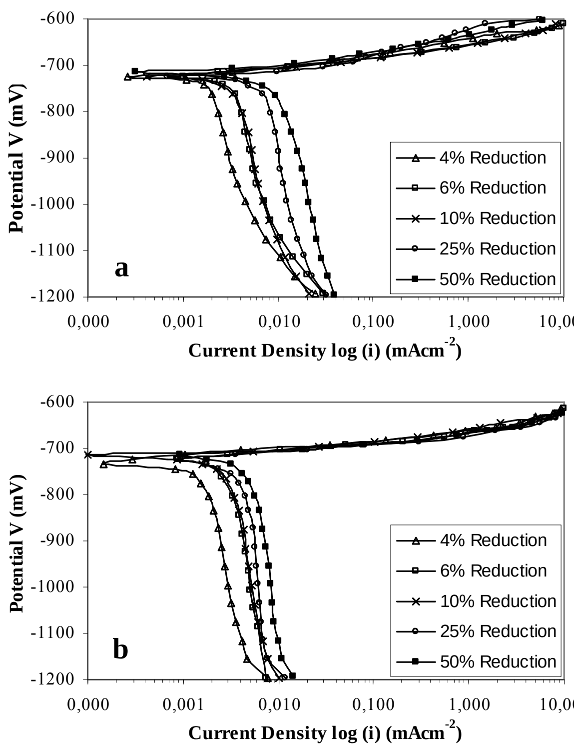

Fig.1. Potentiodynamic polarization curves of a) matrix alloy and b) 20% SiC composite according to cold-worked ratios in aerated 3.5% NaCl solution

The anodic and cathodic polarization curves recorded on matrix alloy and the composites are compared in Fig. 2 in the case of 4 and 25% cold-worked ratio, respectively. The E_{corr}, E_{pit}, i_{corr} values calculated from the polarization curves, carried out in 3.5% NaCl/laboratory atmosphere, are collected in Table 1.

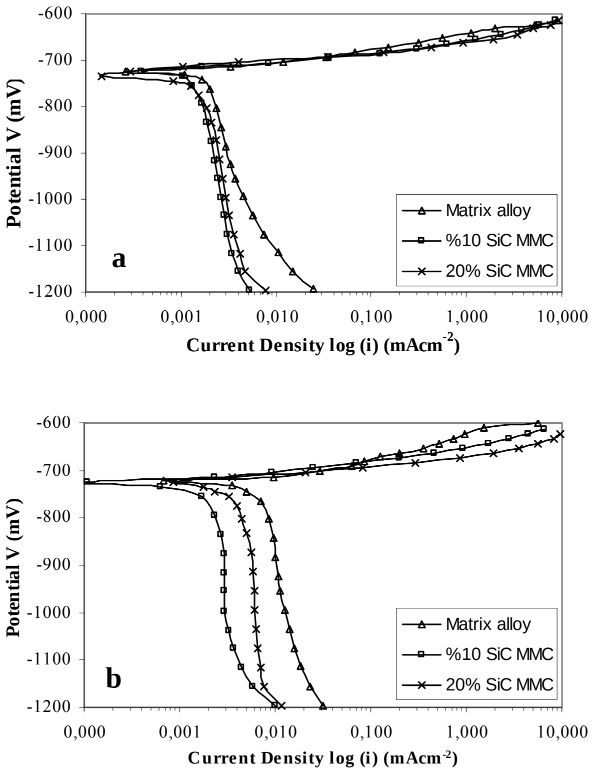

Fig. 2. Potentiodynamic polarization curves of cold-worked materials aerated in a 3.5% NaCl solution a) 4% and b) 25%

Table 1. E_{corr}, E_{pit} and i_{corr} values of the matrix alloy and composites in aerated 3.5% NaCl solution

Material	Reduction (%)	E_{corr} (mV)	E_{pit} (mV)	i_{corr} ($\mu A/cm^2$)
Matrix Alloy	4	-723	-712	2.0
	6	-722	-713	3.1
	10	-722	-713	4.0
	25	-722	-712	8.0
	50	-714	-702	10.0
10% SiC_p	4	-725	-714	1.5
	6	-724	-714	1.5
	10	-715	-704	3.0
	25	-725	-715	2.5
	50	-738	-714	5.0
20% SiC_p	4	-733	-720	1.7
	6	-724	-713	3.0
	10	-714	-705	3.2
	25	-724	-713	4.5
	50	-714	-708	5.5

Table 1 indicates that the corrosion resistances (i_{cor}) of unreinforced matrix alloy and the composites increase with the increase of cold-work level. For example, the average value of the 20% SiC_p composite was calculated to be 3.2μA/cm^2 for the 25% cold-worked specimens (Table 1), which is bigger than for the 4% cold-worked composites (1.7μA/cm^2). Meanwhile, major change in the E_{corr} and E_{pit} values for each composite type were not observed cold working ratio increased from 4 to 50%. Probably, the corrosion potential approaches closely the pitting potential because of subtle polarization effect may be masked by employing aerated solution (Fig. 2). Therefore, in the second stage of the study, all electrochemical tests were repeated under nitrogen atmosphere.

Polarization curves of T8 tempered matrix alloy and 20% SiC composite after deaerated process compare in Fig. 3. In those curves, the pitting potentials (E_{pit}) were demarcated by a marked rise in the anodic current density for the each plastic strain ratio.

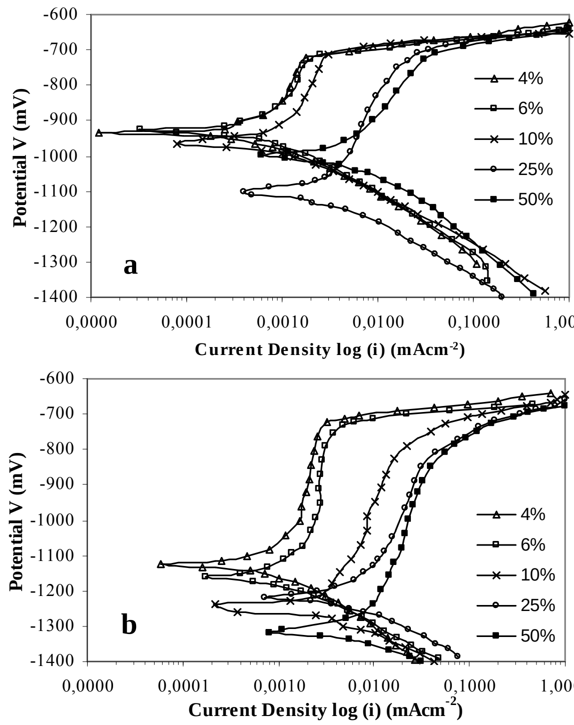

Fig. 3. Potentiodynamic polarization curves of 20% SiC composite according to cold-worked ratios in deaerated 3.5% NaCl solution

Fig. 4 shows the variation of the potentials versus current densities of the materials as a function of SiC particle content for 4 and 25% reduction of cold work. The same as aerated conditions, the E_{corr}, E_{pit}, i_{corr} values calculated from the polarization curves are collected also in Table 2 for nitrogen atmosphere tests.

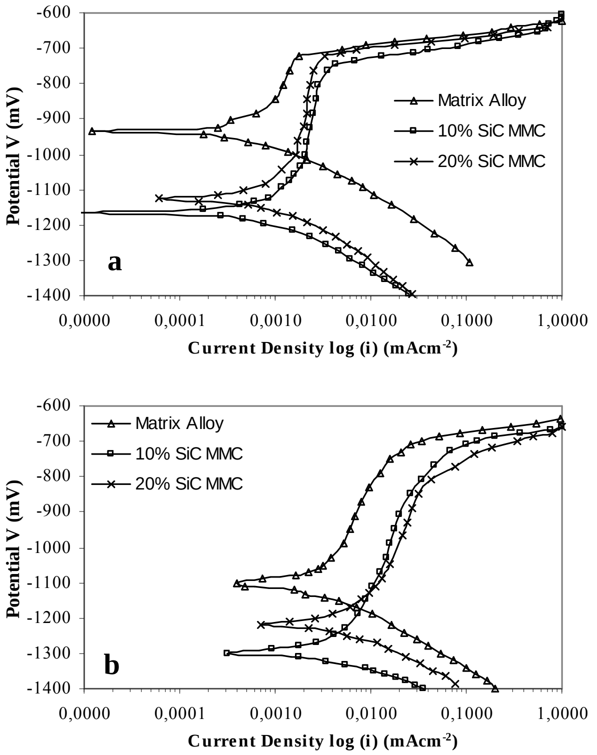

Fig. 4. Potentiodynamic polarization curves of cold-worked materials deaerated in a 3.5% NaCl solution a) 4% and b) 25%

Table 2. Corrosion (E_{corr}), pitting (E_{pit}) potentials and current density (i_{corr}) values of the matrix alloy and composites in deaerated 3.5% NaCl solution

Material	**Reduction (%)**	E_{corr} **(mV)**	E_{pit} **(mV)**	i_{corr} **(μA/cm^2)**
Matrix Alloy	4	-932	-722	0.5
	6	-923	-732	0.6
	10	-964	-712	0.8
	25	-1099	-737	2.6
	50	-999	-737	4.0
10% SiC$_p$	4	-1164	-743	0.8
	6	-1073	-712	1,0
	10	-1108	-746	2.0
	25	-1298	-758	3.0
	50	-1308	-768	5.0
20% SiC$_p$	4	-1123	-743	0.8
	6	-1162	-751	1.0
	10	-1238	-800	2.2
	25	-1219	-817	4.0
	50	-1319	-837	5.9

Table 2 indicates that the i_{corr} values of the composites increase with the increase of cold-work level, whose maximum values reach 4.0, 5.0 and 5.9 μA/cm^2 for matrix alloy, 10%SiC and 20% SiC MMCs, respectively. Briefly, it can be said that the current densities (i_{cor}) of the unreinforced matrix alloy and the composites increased with both increasing SiC particle fraction and cold-worked ratios. In other words, there is a significant coloration between corrosion susceptibility and level of cold work.

Fig. 5 demonstrates the Mg and Si distributions that has been obtained for 25% cold-worked 20% vol. SiC$_p$ composite. The results of X-ray maps show that the concentration of Mg is nearly homogeneous in the matrix alloy (Fig.5-b). But, Si has been observed that preferentially increasing at matrix/SiC particle interfaces (Fig. 5-c).

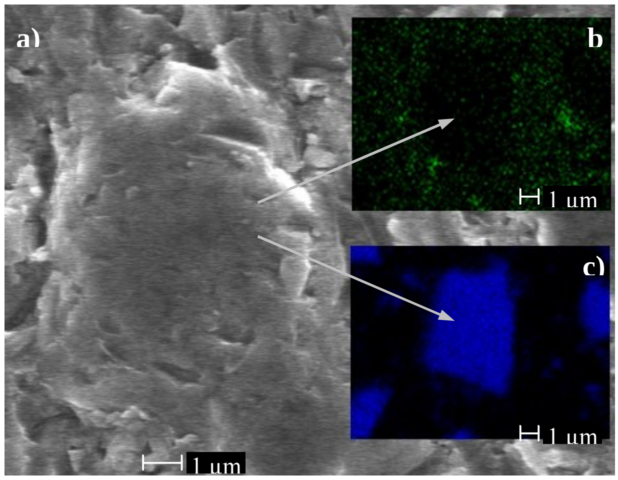

Fig. 5. a) SEM micrograph and X-ray maps of b) Mg, c) Si after T8 temper of the 20% vol. composite

Fig .6 shows the SEM images of the unreinforced matrix alloy and the composites after corrosion tests, which have developed principally localized corrosion at the matrix alloy (Fig. 6-a) and the pitting corrosion at the composites (Fig. 6-b-c).

In composites, the pitting corrosion has propagated principally at the matrix/SiC$_p$ interface (Fig. 7). At the advanced stages of the corrosion, the attack was rather dense around the SiC particles interface (Fig. 8-a). As a result, this kind of attack may affect the normal pitting corrosion behavior of the material. The formation of pits or holes and free facetted silicon carbide due to intensive matrix corrosion is shown in Fig. 8. There is not any indication of corrosion on the SiC$_p$ surface (Fig. 8-b)

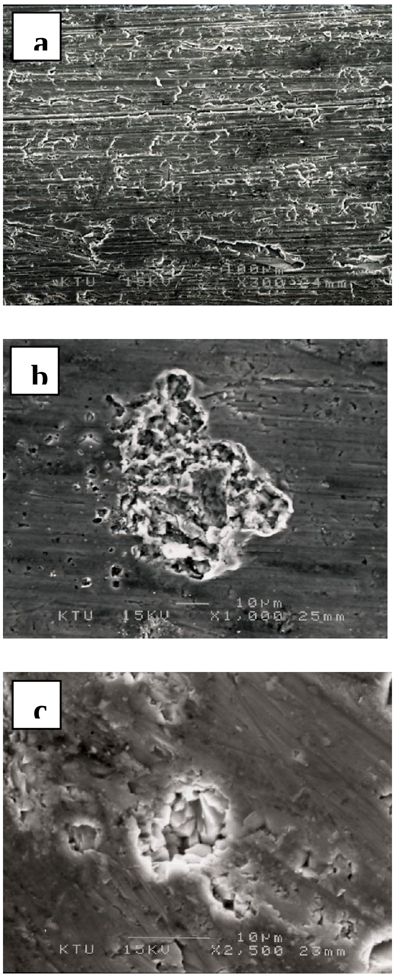

Fig. 6. SEM images of the 25% cold-worked a) matrix alloy and b) 10%, c) 20% vol. SiC composites after corrosion tests

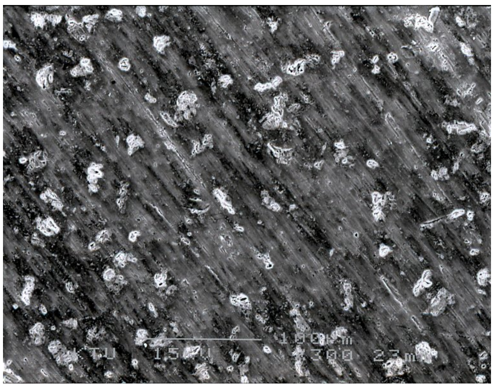

Fig. 7. Preferentially corrosion formed around SiC particles in 4% cold-worked 20% vol. SiCp composite

In our previous studies, XRD results indicated that the Al_4C_3 reaction product was not formed which means a continuous SiO_2 layer is exist on the reinforcement particle surface [9, 18].

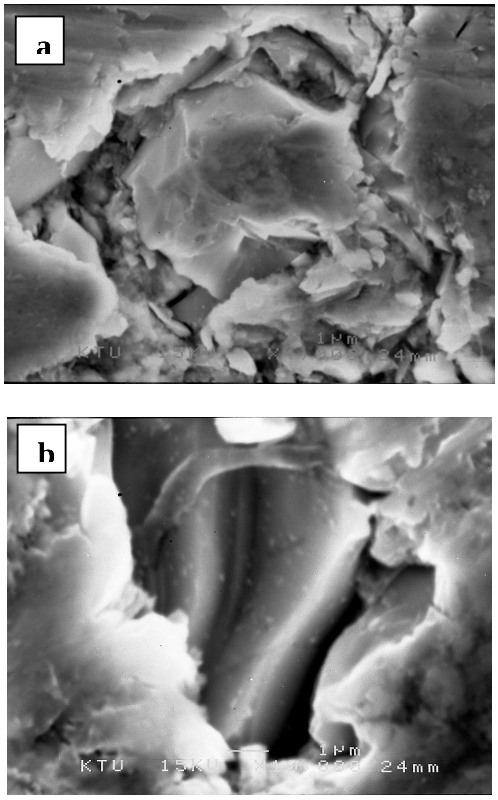

Fig. 8. a) Holes around of SiC particle due to intensive matrix corrosion, b) and free facetted of SiC particle in T8 tempered 20% vol. SiCp composite after corrosion

4. Discussion

Figs 1–4 shown that there is a distinct coloration between the corrosion susceptibilities and cold work levels of the T8 tempered materials. Also, the corrosion resistance of the materials decreases with increasing degree of cold work. In real interface systems, dislocations form at or near the interface to relief the strain energy due to lattice mismatch. According to different authors [3, 19], the reasons of rapid dissolution of atoms in the composite could favour due to the accumulation of a very large dislocation density and high stress concentrations in the Al/SiC interfaces compared to matrix alloy. Therefore, corrosion resistance of AMMCs may be altered SiC particle volume fraction and high dislocation densities formed in the vicinity of SiC particles.

The current density value is directly related to the electrode potential, and it can provide more realistic results related to electrochemical behavior of the composites [20]. In Table 1 and 2, the i_{cor} values of the composites increase markedly with increasing both degree of cold work and SiC volume friction for each material type. There are two important questions in this state, either SiC_p volume fraction or cold-worked ratio may have been altered the corrosion resistance of the composites. Our previous studies [9, 18] indicated that i_{cor} values of the composites are ~0.5µA and 0.8 µA/cm^2 after SiC particle addition and aged heat treatment, respectively. Whereas, increasing the cold-worked ratio increase the i_{corr} values from 0.8 to 5.9 µA/cm^2 in the present study. In other words, the corrosion effect formed owing to cold working is much more than that due to both SiC particle addition and aged heat treatment. The increasing of the i_{corr} values after T8 process may be due to the point defects introduced into the materials by cold working which provide nucleation sites for pits and thus facilitate corrosion. In addition, this would support the mechanism of stress concentration at the interface in the stimulation of the corrosion process [19].

The corrosion attacks may start at Al/SiC interfaces owing to the semi-conducting properties of SiC (Fig. 7 and 8-a). Because SiC_p reinforcement has much higher an electrical resistance (160 Ωm) compared to the A356 alloy (4x10^{-8} Ωm) [12, 21]. Thus, galvanic coupling effect would be possible between SiC and the active the matrix [22]. However, the T8 temper and increasing SiC volume fraction decreased also the size of pits but not their number, as shown in Fig. 6-b-c. These results are in accordance with composite theory because it is well known that SiC particles acting as physical barriers to the pit growing [3, 5, 12, 22]. Consequently, reinforcement and matrix alloy could be the detachment due to applied reduction and the development of a possible crevice effect in T8 conditions (Fig. 8-b) [19].

This illustrates that the decrease in corrosion resistance of the cold worked sample is due to the increased amount of dislocation and point defects introduced into the materials, which serve as high energy sites for the nucleation of pits. In addition, such phenomena can be explained by microcracks and stresses that exist in the composite. Recent studies conducted on the production of MMC indicate that due to the difference in thermal expansion coefficients of the reinforcement (4.5x10^{-6}/K for SiC) and matrix alloy (21.5x10^{-6}/K for A356-T6), some micro-cracks may occur where the discontinuity is present during solidification. The increase in dislocation density around the precipitates outcome from age hardening and residual stresses may increase these micro-cracks. As a result, areas which have different potentials may increase and when the potential exceed E_{corr} value, these areas may act as corrosion nucleation sites [12]. However, it should be expressed that this result is in contradiction with the general point of view that residual stresses and dislocation density are ineffective on the corrosion resistance of Al/SiC composites [3, 12].

Another possible explanation of increased corrosion susceptibility is the distribution of the cracked particles. It is well known that cracked powders possess generally higher surface energy than large particles [23]. The presence of micro-cracked particles can make preferentially corrosion mechanism the corrosion will continue around these particles and also provide the development of main pits. Meanwhile, the structure tends to induce many micro-submicro local batteries, and make the matrix grains potentially differentiate, thus increase the pitting potential. Because, SiC is a noble material and will not undergo corrosion (Fig. 8-b). But this may cause to form the small anode-big cathode corrosion type and the corrosion increase significantly. Thus, localized corrosion in the Al matrix alloy will progress quickly and in depth. This type of corrosion known as "*pitting*" and even it cause less material loss, it may damage the construction. As a result, this kind of constitutions may affect the normal pitting corrosion behavior of the material (Fig. 4-a).

Trowsdale *et. al.* [3] reported that the polarization curves of 50% cold deformed composite were similar to un-deformed composite. This approach was focused only to one deformation ratio. Therefore, it is not said that deformation is not effected corrosion behavior of the AMMCs. Because, it could be seen that the corrosion susceptibilities both of the composites and of unreinforced matrix were increased by increasing the level of cold work even though composites were cold-worked to a plastic strain of 4% in this study.

5. Conclusions

We have performed an experimental study in order to understand the effect of cold working on the corrosion of Al─Si─Mg/SiC MMCs. The following conclusions can be drawn from the above experimental study.

1. The results show that the cold deformation and its ratio have a great effect on the electrochemical behaviors of AMMCs.
2. Deaerated process must be used to determine the tendency of the active metal dissolution in the NaCl solutions.

3. The corrosion parameters calculated from Tafel plot indicates that the corrosion resistances (i_{cor}) of the composites increase with the increase of cold-work level, whose maximum value reach 4.0, 5.0 and 5.9 $\mu A/cm^2$ for matrix alloy, 10%SiC and 20% SiC MMCs, respectively in deaerated 3.5% NaCl solution.
4. The corrosion effect formed owing to cold working is much more than that due to both SiC particle addition and aged heat treatment.
5. The SEM images show preferentially corrosion formed around the SiC particles in the composites (Fig. 8).
6. Both the cathodic behavior of Mg_2Si phase and accelerated precipitation kinetics at Al/TiC interface may reduce i_{corr} current densities of the composites in the T8 conditions.
7. In addition, high dislocation density, residual stresses and micro-cracks may cause to form small anodes thus affect unfavorable the corrosion characteristics.

Acknowledgements

This research project was financed by Ataturk University under BAP 2003/66 in Turkey. The authors would like to thank Prof. Dr. Hanifi Sarac and Prof. Dr. Sinan Yapici for laboratory contribution.

References

[1]. M. Ferry and P. R. Munroe, Recrystallization kinetics and final grain size in a cold rolled particulate reinforced Al-based MMC, Composites Part A: Applied Science and Manufacturing, Volume 35, Issue 9, September 2004, Pages 1017-1025.

[2]. David Talbot, James Talbot, Corrosion Science and Technology, ch.5-9, CRC Press, Boca Raton, Florida, 2000.

[3]. Trowsdale, A.J., Noble, B., Haris, S.J., Gibbins, I.S.R., Thompson, G.E., and Wood G.C., The influence of silicon carbide reinforcement on the pitting behaviour of aluminium., Corrosion Science, 38 (2), 1996, 177-191.

[4]. Trzaskoma, P.P., Pit morphology of aluminum alloy and silicon carbide/aluminum alloy metal matrix composites, Corrosion, 46(5), 1990, 402-409.

[5]. Trzaskoma, P.P., McCafferty, E., Crowe, C.R., Corrosion Behavior of SiC/Al Metal Matrix Composites., Elektrochemical Society of Journal, 130(9), 1983, 1804-1809.

[6]. G. K. Quainoo, S. Yannacopoulos, The effect of cold work on the precipitation kinetics of Al6111 aluminum, Journal of materials Science, 39, 2004, 6495-6502.

[7]. Liu, Y.L., Hansen, N., Jensen, D.Juul, Recrystallization microstructure in cold-rolled aluminum composites reinforced by silicon carbide whiskers, Metallurgical transactions. A, Physical metallurgy and materials science, Volume 20 A, Issue 9, September 1989, Pages 1743-1753.

[8]. C. Tekmen, U. Cocen, Role of cold work and SiC volume fraction on accelerated age hardening behavior of Al Si Mg/SiC composites, Journal of Materials Science Letters 22, 2003, 1247 – 1249.

[9]. B. Dikici, M. Gavgali, and C. Tekmen, Corrosion Behavior of an Artificially Aged (T6) Al–Si–Mg-based Metal Matrix Composite, Journal of Composite Materials 2006 40: 1259-1269.

[10]. De Salazar, J.M.G., Urena, A., Manzanedo, S., Barrena, M.I, Corrosion behaviour of AA6061 and AA7005 reinforced with Al_2O_3 particles in aerated 3.5% chloride solutions: potentiodynamic measurements and microstructure evaluation, Corrosion Science, 41, 1999, 529-545.

[11]. Shreih, L.L., Corrosion. Tien Wah Pres (Pte) Ltd., 1, 4:3-4:30, Singapore.,1979

[12]. Lucas, K.A., and Clarke, H., Corrosion of Aluminium-based Metal Matrix Compoites. Research Studies Pres Ltd, p.1-137, England, 1993.

[13]. Yaghmaee, M.S., and Kaptay, G., On the stability range of SiC in ternary liquid Al-Si-Mg alloy. Materials Worlds, Proceeding of Hungarian Materials Science Society, Proceeding of Hungarian Materials Science Society, e-journal:http://materialworld.fw.hu, 2(3), 2001.

[14]. Lloyd, D.J. The Solidification Microstructure of Particulate Reinforced Aluminium/SiC Composites, Composites Science and Technology 35,159-16, 1988.

[15]. C. Tekmen and U. Cocen, The Effect of Si and Mg on Age Hardening Behavior of Al-SiCp

Composites, Journal of Composite Materials 2003 37: 1791-1800
[16]. ASTM G1-90, Standard Practice for Preparing, Cleaning, and Evaluating Corrosion Test Specimens, ASTM International. USA, 15-20, 03.02, 2001.
[17]. ASTM G5-94, Standard Reference Test Method for Making Potentiostatic and Potentiodynamic Anodic Polarization Measurements, ASTM International. USA, 58-69, 03.02, 2001.
[18]. Gavgali, M., Dikici, B., Tekmen, C., "The effect of SiCp reinforcement on the corrosion behaviour of Al based metal matrix composites", Corrosion Reviews, vol. 24 (1-2), 27-37, 2006.
[19]. C. Monticelli, F. Zucchi, G. Brunoro and G. Trabanelli, Stress corrosion cracking behaviour of some aluminium-based metal matrix composites, Corrosion Science, Volume 39, Issues 10-11, October-November 1997, Pages 1949-1963
[20]. J.R. Galvele, Tafel's law in pitting corrosion and crevice corrosion susceptibility Corrosion Science, Volume 47, Issue 12, December 2005, Pages 3053-3067.
[21]. ASM Handbook, ASM International, 2, 1-215, Ohio/USA, 1990
[22]. Turnbull, A., Review of corrosion studies on aluminium metal matrix composites. British Corrosion Journal, 27(1), 27-35, 1992.
[23]. Aiju Li, Yuhua Zhen, Qiang Yin, Laipeng Ma and Yansheng Yin, Microstructure and properties of (SiC, TiB_2)/B_4C composites by reaction hot pressing, Ceramics International, Volume 32, Issue 8, December 2006, Pages 849-856.